Implications of Underdamped Stepper Mechanism Performance and Damping Solution Methodology

Shane Brown* and Scott Starin*

Abstract

When driving a stepper motor the control method of stepping the motor has a significant impact on the performance of the mechanism. When driving a stepper motor system with unipolar or wave method of control, the back-emf generated in the open, unregulated coil creates a stepper motor system that provides significantly less inherent damping compared to full bipolar control. Less damping results in higher overshoot, ringing, and potentially exciting mechanical resonances resulting in fatigue. In addition, a significantly underdamped system, particularly with significant load inertia, raises many concerns with mechanism life and performance. The mechanism described herein utilizes a Rotary Accelerometer (RA) for step counting as well as state-of-health monitoring [1]. Another consequence of an underdamped mechanism using accelerometers is that the RA data is of limited or no value, due to high overshoot acceleration. This paper presents a proven design approach to damp a stepper motor driven in a unipolar, wave fashion, or a system with significant inertia mismatch between the motor and the reflected load.

Introduction

Ball Aerospace & Technologies Corp. (BATC) is involved in a proprietary space vehicle application that has several mechanisms. One of the mission critical applications is a single degree of freedom mechanism consisting of a geared stepper motor actuator coupled to a balanced load inertia, to be referred to here after as the mechanism. The load of the mechanism must be controlled to precision interval locations and have full 360° of operation (no hard stops). A geared stepper motor was selected because of the precision response, simple controls, and proven heritage and reliability.

For various reasons, a three-phase stepper motor with an integral Rotary Accelerometer (RA) was selected for the actuator. We believed the mechanism was simple enough that an Engineering Development Unit (EDU) was not required. However, for calibration of the control electronics, a representative EDU mechanism was produced simultaneously with the flight hardware. During the electronics calibration procedure anomalous performance of the mechanism was observed, resulting in the inability of the control electronics to process the RA feedback signal as originally intended. We believed the erratic performance of the mechanism was a mechanical reliability concern, due to significant overshoot, operational resonance and mechanical ringing.

This paper details the troubleshooting, analysis and test simulation process, as well as the ultimate course of action taken to resolve the performance issue. We also detail the implications of the stepper motor drive control methods and the effects they have on mechanism performance. In addition, we detail the requirements for interfacing with, and signal processing of, the RA signal for step verification. Time was critical in the decision making and rework process because flight hardware was received, and all viable solution options required an in-process modification to the flight hardware. Because of these schedule needs, several solutions that would have been plausible for the initial design phase, were no longer viable, and are not fully discussed in this paper.

The Mechanism

Mechanical Description

The mechanism drive system consists of a three-phase stepper motor with an integral RA and gear-head with a 96:1 gear ratio (N). The gear-motor is coupled to a drive shaft with a flexible coupling. Both the motor and the drive shaft are secured to the flexible coupling with match drilled pins. A preloaded,

* Ball Aerospace & Technologies Corp., Boulder CO

Proceedings of the 39th Aerospace Mechanisms Symposium, NASA Marshall Space Flight Center, May 7-9, 2008

separated bearing pair supports the drive shaft; and the drive shaft in turn supports the balanced load inertia. Because the load is balanced, the detent torque of the stepper motor is sufficient to hold the load in place during launch and no launch lock is necessary. **Figure 1** below shows a schematic of the drive system.

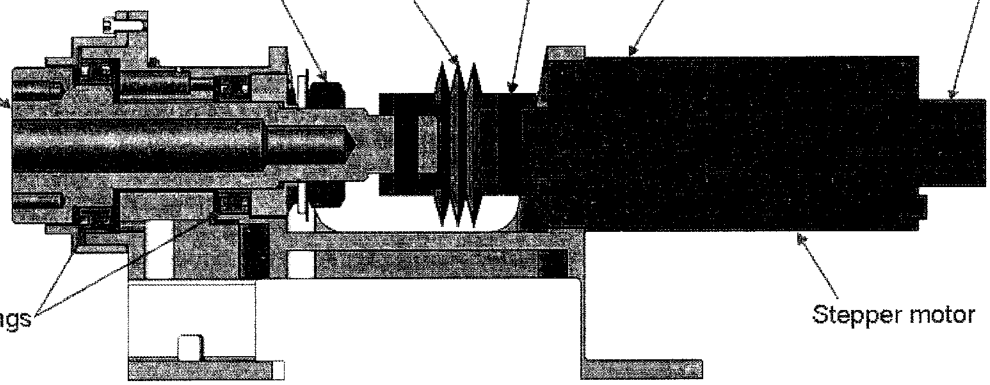

Figure 1: The Drive

The total mass of the suspended load is 1.36 kg and the mass moment of inertia of this rotating load (J_L) is 0.027 kg*m^2. When reflected through the gear-head, the load inertia (J_{LM}) [3] is:

$$J_{LM} = (J_L) / N^2 = (0.027 \text{ kg*m}^2) / 96^2 = 2.9 \times 10^{-6} \text{ kg}\bullet\text{m}^2 \quad (1)$$

The mass moment of inertia of the 1.5 inch diameter stepper motor (J_M) is 2.8 X 10^{-5} kg•m^2. The inertia factor (J_F) [3] is defined as:

$$J_F = (J_M + J_{LM}) / J_M \quad (2)$$

For this system the inertia factor is 2.64. A good rule of thumb is that the inertia factor of a stepper motor system should be less than three. Additionally, torque margin was calculated to be 126% using a factor of 3 for all friction values, meeting the MIL-A-83577 requirement of 125% for mechanism at their Critical Design Review. Analysis indicated a functional design.

Position Knowledge:

Several options were considered to provide rotational feedback of the mechanism, including contacting and non-contacting switches, encoders, potentiometers and RAs. Contacting switches were ruled out because they are inherently limited life items, while encoders and potentiometers were eliminated because of their relatively large size. The RA was selected over the non-contacting switches, such as Hall Effect sensors, because the RA was easier to mechanically integrate to the system since it is integral to the motor, requires fewer lead wires, has higher reliability numbers, higher positional knowledge and is easier for software to implement. The RA provides the added feature of monitoring the heath of the drive system. If the peak acceleration decreases, the drive is degrading; and this knowledge can enable the operations team to modify their use of an on orbit mechanism before it fails. A technical disadvantage of using a RA for feedback is that it derives position of the motor shaft, not the output of the gear-head shaft. As a result the accuracy of the position feedback provided by the RA is limited by the backlash of the gear-head, which for our application was sufficient for positional knowledge. There is also a procurement disadvantage, as the technology is patented by CDA InterCorp, and thus is only available from one supplier. There are other suppliers with acceleration feedback technology, but they require DC excitation, which results in additional power loss and performance variation with supply voltage fluctuations.

EDU Performance

The EDU was necessary for calibrating and determining the gains in the electronics to determine proper step verification. More on this process will be discussed later in the paper. The Responsible Engineer for the control electronics observed the proper direction of rotation and displacement for stepping the actuator, however, the observed output of the RA showed significant overshoot and ringing of the stepper motor. Figure 2 below shows the RA output from a single step of this development unit.

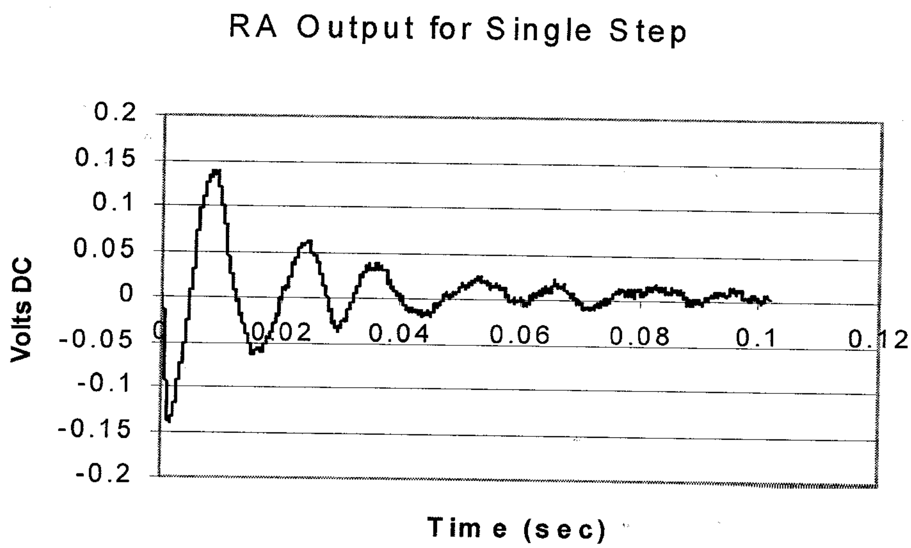

Figure 2. Oscilloscope Output of the Underdamped EDU Mechanism

This plot of data captured with an oscilloscope shows the significant overshoot and ringing of the mechanism. Figure 3 below shows the RA output of 6 steps being driven at the operational pulse rate of 26 Pulses Per Second (PPS).

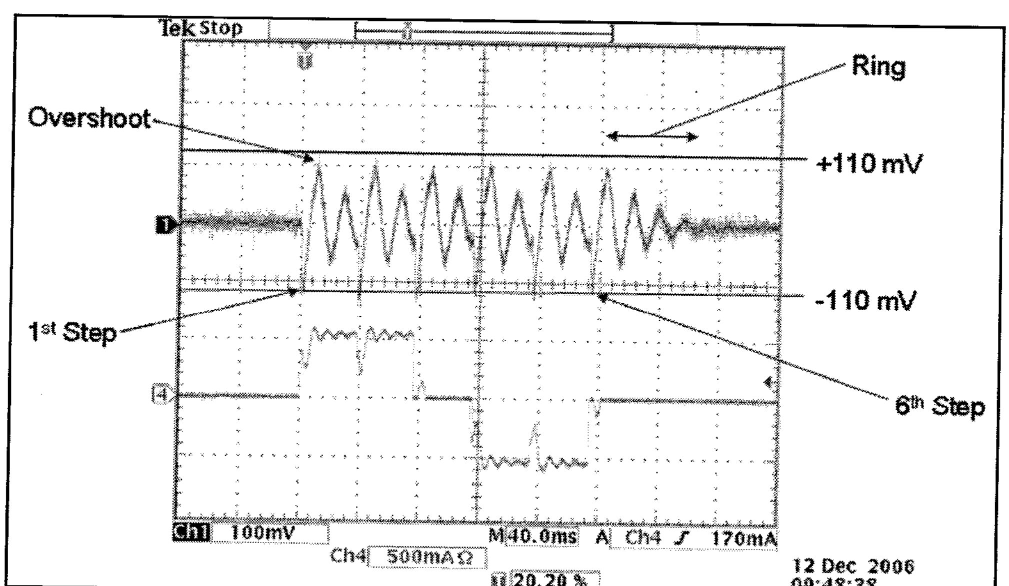

Figure 3. Six Steps at the Operational Pulse Rate of 26 PPS

This oscilloscope trace shows that the motion of the mechanism was erratic and significantly underdamped. The ringing was both audible and visible in the lab, raising the concern that loads might be centered on if a resonance was excited a bearing retainer could fail, or the gears could micro-pit due to the vibration and reversing. Also problematic in this performance was that the overshoot acceleration voltage was nearly equal to the primary step voltage. Our "Original Transition Voltage Counting" method planned yielded false positional information as the threshold voltage is realized at the primary step as well as the overshoot. The processed logic would falsely determine the motor was simply stepping back-and-forth between two pulses. (Original Transition Voltage Counting is described in the later section Processing the Rotary Accelerometer Signal.)

Investigation of the Problem

ERB Process:
Due to schedule constraints, EDU testing and flight assembly occurred concurrently. At the time, the EDU testing showed that the designed method for step verification did not work as intended, the flight stepper motor had already been received, almost all of the mechanisms piece parts had been completed and the flight electronics were in fabrication. Re-work of flight hardware was going to be required to solve this problem. An ERB was convened to determine the best system solution for the program. The first step in the ERB process was to brainstorm every possible root cause. **Figure 4** shows the fishbone diagram developed by the ERB team as a result of this brainstorming effort.

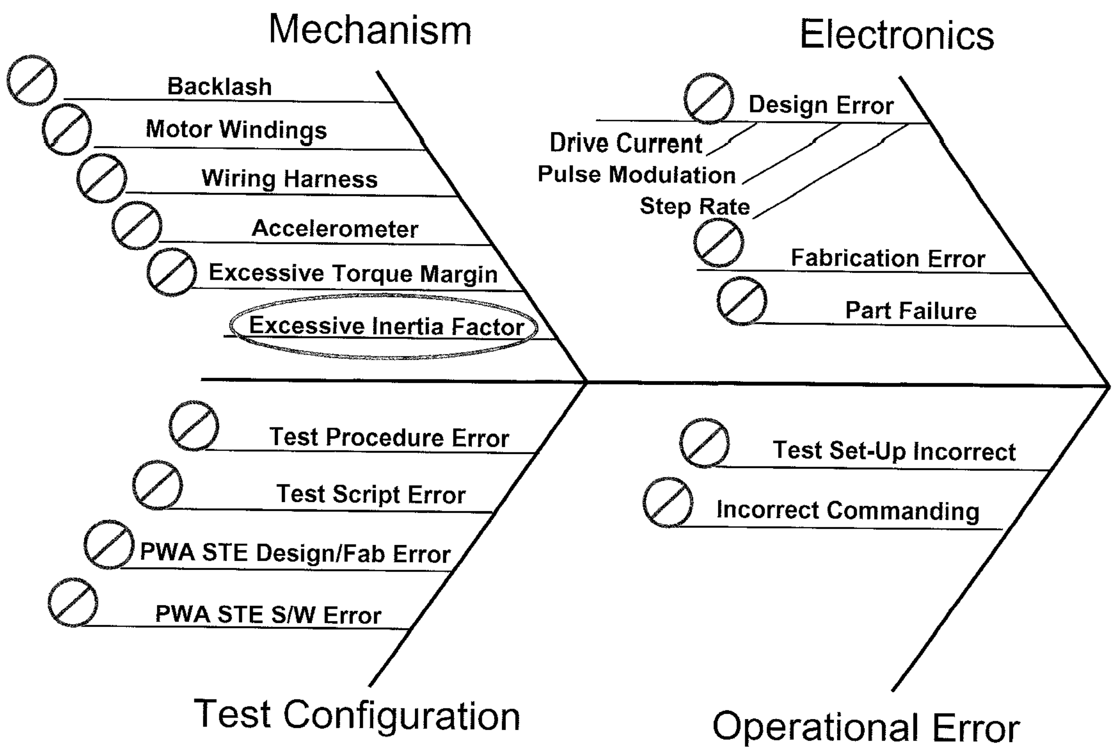

Figure 4: ERB Fishbone Diagram

An audit of the EDU electronics and Special Test Equipment's documentation and certification logs determined the electronics were built to print and certified. Review of the test procedure and set-up eliminated the test procedure and operator error. Review of test data supplied by the motor supplier eliminated backlash, motor windings and the accelerometer. A pin to pin test of the wire harness verified its manufacture. Torque margin of the EDU was measured using the RA to be greater than 400%, however, when a reduced voltage was applied to the EDU the system still exhibited significantly underdamped actuation. Therefore, excessive torque margin was eliminated. While the inertial factor of 2.64 was below the desired value of three, because the rotating mass was so large, at 1.36 kg, the initial determination of the ERB was that the system was under-damped because the inertia factor was too high, and the trade table of solutions for this problem was created.

A Note On Torque Margin

Torque margin is measured using an RA by increasing the load friction until the drive begins to miss steps; the ratio between the nominal RA output and the RA output when a step is missed is the torque margin [1]. For the measurements made using the EDU, the load inertia was increased by applying hand pressure to the rotating load, and an operational torque margin of greater than 400% was measured. The calculated torque margin at CDR was estimated to be 126%. This large discrepancy between the calculated and actual margins is a result of performance projection without hardware to empirically test our CDR analysis. Standards require the assumption of worst case gear-head efficiency, motor detent torque, and most significantly a factor of safety on all friction values. This is sufficient justification for using EDUs early in a system's development. Actual torque margin measurements can be made, potentially enabling the use of a smaller stepper motor or increasing efficiency by reducing power consumption.

Troubleshooting and Root Cause Determination

Table 1 below delineates the trades considered for solving the excessive inertia factor problem. We sought the most technically robust solution that minimized cost and schedule impacts to the program. The trades were complicated by the fact that both flight and EDU hardware were in house, and any change to the mechanical configuration required an in-process change to existing hardware.

Table 1. Trade Consideration Table

Area	Modification	Advantages	Disadvantages
Electrical	Use RA to produce contour current.	No change to mechanism. Lowest risk option.	Significant changes to electronics to add compensation network.
Electrical	Increase or decrease step rate to optimize stepping characteristic.	No change to mechanism, "only" FPGA modification.	Does not solve mechanical resonance problem.
Electrical	Contour pulse waveform to attenuate acceleration (Miller effect)	No change to mechanism.	Significant power loss increase, minimal performance advantage.
Electrical	Modify pulse verification logic to ignore overshoot pulse.	No change to mechanism, "only" FPGA modification.	Does not solve mechanical resonance problem.
Electrical	Short Redundant windings while primary is operated (and vice versa)	Minor electronics change	If relays or open winding failure underdamped situation would persist.
Electrical	Add delta configuration load resistors across bridge to provide inherent damping.	No change to mechanism.	Board layout modification required to accommodate large power resistors. Increase in power loss on board.
Mechanical	Increase gear ratio (N) to minimize Inertia Factor	Not many.	Modify mechanism hardware and electronics FPGAs. System velocity requirements could not tolerate slower operation.
Mechanical	Reduce load inertia to minimize Inertia Factor	No change to electronics or software	Significant modification to mechanism with minimal performance benefits.
Mechanical	Modify winding configuration to Delta.	No change to electronics or software	Requires in-process upgrade of EDU and Flight hardware. If motor winding opens, damping benefit lost.
Mechanical	Add Shorted Coils in Motor to approach critical damping	No change to electronics or software	Requires in-process upgrade of EDU and Flight hardware

The first three mechanical solutions were quickly eliminated because the change would violate other operational requirements. Using the RA contour current was also quickly removed from the trade space because of the significant changes required to the electronics. This method uses the motor peak acceleration to attenuate the supply voltage or current. [5]. While this is the "elegant" solution, and the circuitry is relatively simple, a modification to the board layout and the additional tuning required was schedule prohibitive. The best solution, from a cost and schedule standpoint, was changing the step rate to optimize stepping characteristics, so this was tested first.

Decreasing the pulse rate did not change the overall performance of the system, and was thus eliminated, but increasing the pulse rate did yield some interesting results. It was found that the system did have a "sweet spot" at half the resonance of the ringing, approximately 64 Hz. If the system was driven at 64 PPS, each subsequent step coupled with the bounce of the previous step. See Figure 5. However, this solution was eliminated for two reasons: First, it would require a late modification of the flight FPGA once the flight mechanism had been built and its resonance determined; second, the difference between the peak voltage of the first step and the subsequent overshoots was too small. The threshold voltage is determined by a resistor, and as this resistor drifts due to temperature changes and/or end of life degradation the threshold voltage will drift accordingly. Our analysis showed that we needed a much greater delta between the peaks of the pulse and the overshoot.

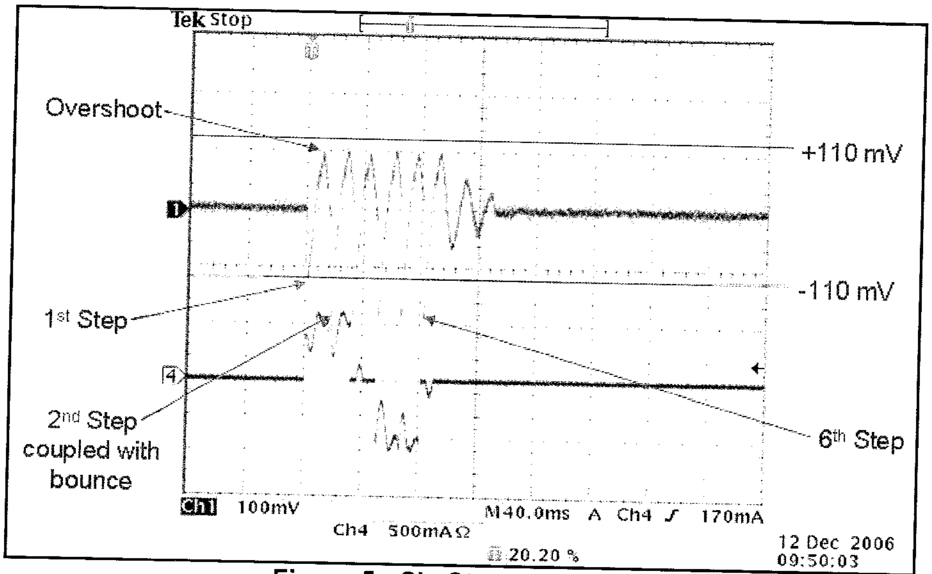

Figure 5: Six Steps at 64 PPS

Another interesting result was that when the system was driven faster than half the resonance of the ringing the amplitude of the acceleration of the second step decreased. See **Figure 6**. This behavior was consistent for all rates greater than 64 PPS. Finally, if the system was driven at any rate between the operational pulse rate of 26 PPS and the sweet spot of 64 PPS, the only change was that there were fewer bounces the closer the rate got to 64 PPS, but going slower than 26 PPS, the overall system performance did not change.

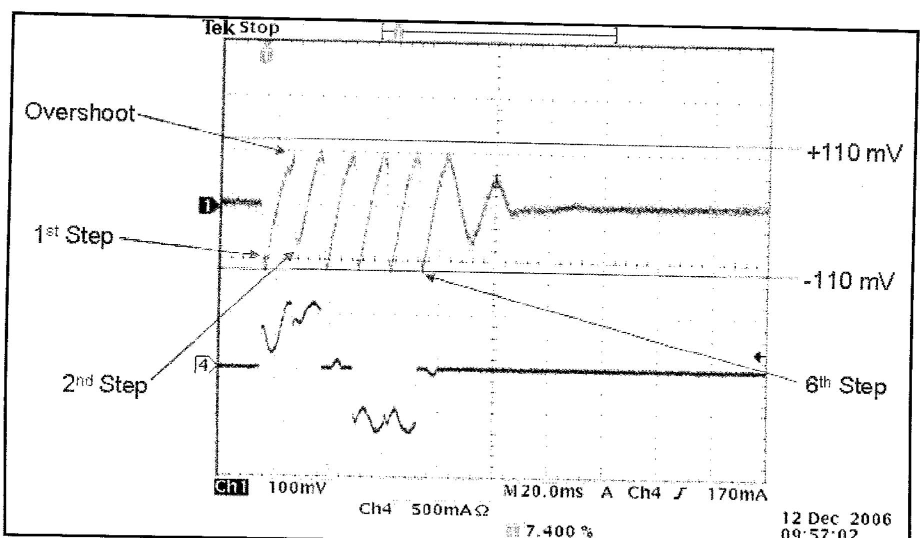

Figure 6: Six Steps at 92 PPS

The next best, solution from a cost and schedule standpoint, was minor modification of the electronics, therefore our testing moved onto shaping the pulse to reduce the acceleration. One of the modifications tested was to add large capacitors to the drive circuitry to "soften" the edges of the voltage pulses. This technique is known as the "Miller Effect". Several one µF capacitors were added, and while there was some benefit to the mechanical resonance, the underdamped situation still persisted. Also power losses on the electronics board increased, and there was no "real estate" on the board to add the sizable capacitors. Therefore, this option was eliminated. This, and other methods, did reduce the audible noise on the electronics board increased, and there was no "real estate" on the board to add the sizable capacitors. Therefore, this option was eliminated. This, and other methods, did reduce the audible noise of the system, but all still resulted in insufficient difference between the pulse and overshoot signals of the RA, and we still had a concern about mechanism fatigue.

The final step of testing was to run the drive with the load inertia removed. When this was done, there was no change in the performance of the system. This was the "Ah-ha!" moment of our testing. Our initial most probable root cause was incorrect, for if the system had an excessive inertia factor, removing the load inertia would have solved the problem. We now realized that we had an underdamped stepper motor system and believed our wave drive method was the root cause. To validate our new root cause we shorted the redundant winding of the EDU by tying the three redundant lead wires together. With the shorted windings we now had the critically damped system that we had originally expected based on component level testing of the stepper motor by the supplier. While we had known that the supplier had performed their component level testing of the stepper motor using a bi-polar driver, we had not understood the implications of our different drive methods. (Wave and bi-polar drive methods are described in the later section Method of Three-Phase Control.)

Homing in on the Solution

Three methods of damping the system were evaluated. The first was modifying the electronics to short the redundant side windings when driving with the primary side and to short the primary side windings when driving with the redundant side. The system requirement that the mechanism be one fault tolerant eliminated this solution. If one of the primary windings failed open, causing the system to switch to the redundant side, the damaged primary windings would be unable to provide the required damping.

The second was adding delta configuration load resistors across the bridge to provide damping. This method was ruled out because it required a new layout of the printed wire assembly to accommodate the large load resistors. The added power loss on the board was also a disadvantage. However, empirical testing of various load resistors across the redundant winding allowed us to determine the magnitude of damping desired to achieve adequate damping and robust step counting.

This left us with our final option, developing a new motor with additional shorted coils that would act as an integral eddy current damper. This solution had the advantage of being transparent to the electronics, but it did have significant cost and schedule ramifications for the mechanism. Schedule issues were alleviated by changing the assembly sequence of the mechanism. Communication provided by the ERB process kept program management and effected disciplines informed and participating in the decision making process. Cost impacts were understood and accepted.

The Solution

Calculated Solution

Once we decided to incorporate the internal damping via redundant shorted coils, we needed to revise the motor torque constant and determine the requirements for the shorted damping coils. From EDU actuator torque margin testing with the RA, we determined we could reduce the motor torque by 50% and still be well above the 100% torque margin required for flight hardware by AIAA S-114-2005. From the shorted load resistor testing conducted, we determined that the mechanism required at least 15% of a fully shorted winding to provide enough damping for reliable stepping and robust RA signal processing.

The EDU motor had the following performance criteria for primary and redundant:

- Motor Torque Constant (Kt) = 0.205 Nm/Amp
- Winding Resistance (Ω) = 40 Ohms
- Motor Constant (Km) = 0.0324 Nm/$\sqrt{}$watt
- Holding Torque at Minimum Voltage (Th) = 0.092 Nm
- Damping Rate with fully shorted redundant windings (Bm) = 1.048 X 10^{-3} Nm-sec/rad

One of the many advantages of working in SI units is the simple determination of the damping rate of a motor with shorted coils. The damping rate is equal to the motor constant, squared, if units are Nm/$\sqrt{}$watt ($Bm = Km^2$) [2]. This first order relationship is applicable for shorted alternator analysis. The equation becomes more complicated at high velocities, but for applications where the rotor velocity is below 200 rad/sec, this relationship is valid.

$$Bm \approx Km^2 \qquad (3)$$

Armed with this information, we calculated what winding modifications were required to achieve reduced holding torque and increased damping, by adding a separate set of shorted windings. The reduction of one gage of magnet wire reduces the volume of the turns and increases DC Resistance by 26%. Since we wanted to reduce torque constant as well, we needed to reduce the number of turns into the motor phases. A straight reduction in turns will reduce the torque constant by the same percentage. **Table 2** describes the original EDU performance (EDU#1) and our desired "New" motor performance.

Table 2: Motor Design Characteristics Comparison

Parameter	Units	EDU#1 (Baseline)	"New" Motor (EDU#2 & Flight)	Comment
Torque Constant	Nm/Amp	0.205	0.164	20% Reduction in Number of Turns = 20% reduction in torque constant.
Turns Reference	Reference	100%	80%	
Winding Resistance	Ohms	40	45	Use magnet wire size 1.5 AWG finer than baseline
Percentage Pack for power windings	%	100 Ref	57%	20% less turns, and 1.5 gage finer wire ($100*0.8*1.26^{-1.5}$)
Motor Constant	Nm/√watt	0.0324	0.0244	Kt / √R
Holding Torque at 18 VDC	Nm	0.092	0.066	~30% reduction in torque desirable.
Stall Power at 35 VDC	Watts	30.6	27.2	~10% reduction in power

Reducing the power winding pack (slot fill percentage) to 57% of EDU#1, allows us to use up to 43% of the slot area as shorted coil damping windings. **Table 3** compares the shorted coil requirements and performance to the power winding for EDU#2 and Flight versions.

Table 3: EDU#2 & Flight Motor Performance Relative to EDU#1

Parameter	Units	Power Winding	Shorted Coil	Comment
Turns Reference (Percentage of EDU#1 turns)	Reference	80%	80%	Use same percentage of turns on shorted coils as primary power. Note: This is not a requirement.
Resistance	Ohms	45	63	1.5 wire sizes finer than the power winding. ($45*1.26^{1.5}$).
Motor Constant	Nm/√watt	0.0244	0.02066 Ref.	Reference only, used to calculate damping rate.
Shorted Coil Damping Rate	Nm-sec/rad	N/A	4.27×10^{-4}	Two sets of damping coils working together.
Percentage Pack of EDU#1 Slot Fill	Ref	57%	40%	Providing an overall slot fill of 97% of EDU#1.

All of our desired characteristics are met with this scenario. The torque margin reduces from 400% to 214% with the new proposed motor, and the damping rate with the shorted coils is 40% of a fully shorted redundant winding. If there is a failure of one set of coils, the damping rate will be 20% of a fully shorted winding set, still within our desired requirements, so our new motor is one fault tolerant. Since we have sufficient of torque margin, we wanted to add as much damping as possible.

shorting resistors across the redundant winding to simulate the magnitude of damping of the "New" motor's shorted windings. Figure 7 below shows a scope trace of our test set simulation. This plot shows significant difference between the primary pulse RA signal and the overshoot. Additionally, the mechanical performance of the system was adequately damped and torque margins were exactly as predicted from the previous analysis.

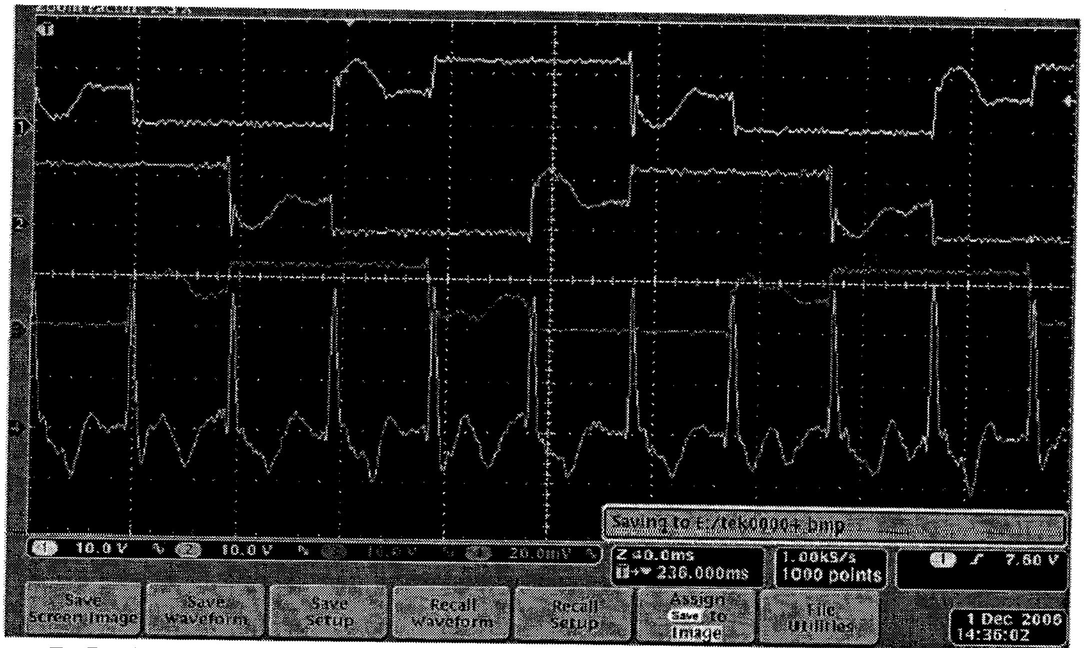

Figure 7. Performance Simulation of the Stepper Motor with Integral Eddy Current Damper

Step Performance Simulation

Stepper motors perform like classical underdamped second order systems. It is a straightforward procedure to analyze the RA output to determine the step kinematics of a mechanism by varying the Damping Ratio (ζ) and time factor ($\Delta\tau$) of classical second order response equations. This allows us to correlate actual performance to theoretical step performance.

Motor position (θm) of a second order response system may be simulated from the following equation [4]:

$$\theta m_t = \mathrm{E}\left[1 - \frac{e^{-\zeta \bullet t}}{\beta} \bullet \sin(\beta t + \phi)\right] \quad \text{.......(4)}$$

Where:

- θm_t = Motor Position at time "t" in radians
- E = Step Angle in radians
- ζ = Damping Ratio (dimensionless $0<\zeta<1$)

$$\beta = \sqrt{1-\zeta^2} \quad \text{.......(5)}$$

$$\phi = \cos^{-1}(\zeta) \quad \text{.......(6)}$$

$$\psi = \tan^{-1}\left(\frac{\zeta}{\sqrt{1-\zeta^2}}\right) \quad \text{.......(7)}$$

Equation 4 is a time-normalized equation. You may establish a new time base by varying a "time factor" ($\Delta\tau$). Simply vary the time base of the simulation to achieve an equivalent crossover time as observed from the empirical data. You may then calculate the velocity (ω) by taking the derivative of position with respect to time ($d\theta/dt$), and the acceleration by taking the derivative of velocity with respect to time ($d\omega/dt$). Vary ζ and $\Delta\tau$ in our spreadsheet until our model matches the observed acceleration data from the RA. From this process, we have detailed kinematical position, velocity and acceleration information of the mechanism simply by matching the model to the observed acceleration signals.

Referring back to **Figure 2**, the oscilloscope output of EDU#1 for a single step of the mechanism with load inertia, in order to simulate the performance, we used the equations above to match the overshoot and settling characteristics. **Figure 8**, is our simulation with the damping ratio and time factor noted.

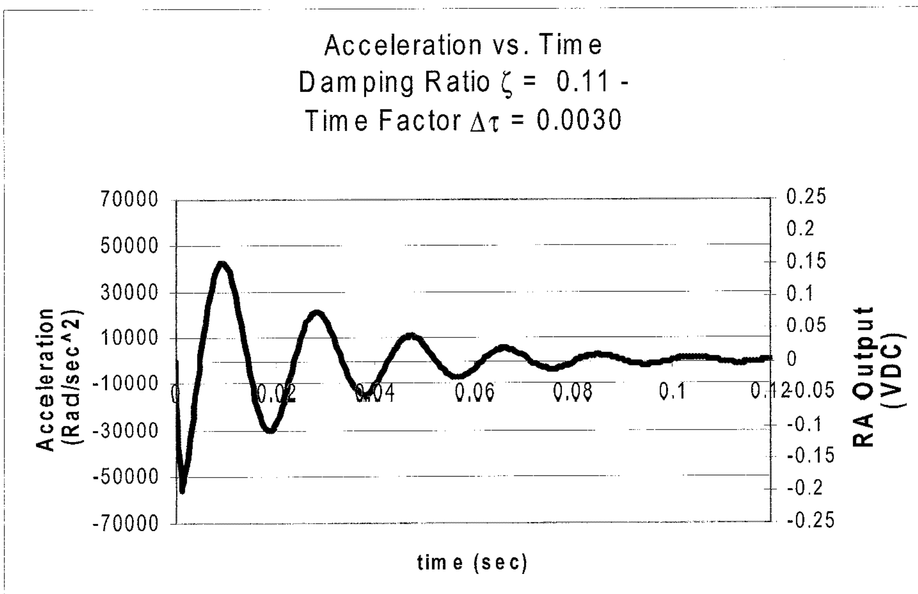

Figure 8: Simulation of EDU#1 Acceleration Profile

<u>EDU / Flight Modifications:</u>
The elegance of this design change was that it was transparent to the rest of the system, both mechanical and electrical. The new motor had the same electrical interface and would be controlled as originally planned. The new motor had the same mechanical interface, the same envelope and would meet our torque margin requirements. Additionally, in order to minimize both the cost of and the time to fabricate the new flight motors, the existing flight motors' gear-heads were reused. The performance of the motor supplier, CDA InterCorp, during this re-build effort was extraordinary: delivering two flight motors only eight weeks after the contract was signed. The total time from discovery of the problem until the new motors were received was just under five months. Because other parts of the assembly were able to proceed in parallel, the actual schedule delay to the mechanism was only two months. The program was able to plan accordingly and there was no impact to the overall system schedule.

<u>Modified Actuator Performance:</u>
The modified actuators with integral eddy current damping performed better than expected. The magnitude of the acceleration, measured torque and inherently damped characteristics were as predicted, or better than predictions. The scope shot in **Figure 9** below shows the motor phase voltages along with the new mechanism acceleration profile, with the internal damping. Notice how the RA signal shows a distinct pulse per step with minimal overshoot providing desired monitoring chrematistics. Robust acceleration characteristics, minimal overshoot and consistent performance highlights the improved mechanism. This scope trace was taken at nominal voltage (+24VDC) and pulse rate. The acceleration signal is raw and unfiltered. The difference between the overshoot pulse and the first transient pulse is a robust 400%, making the step counting reliable and consistent. Most importantly, the stepping characteristic was smooth, quiet and dependable. The erratic motion and audible rattle was no longer present.

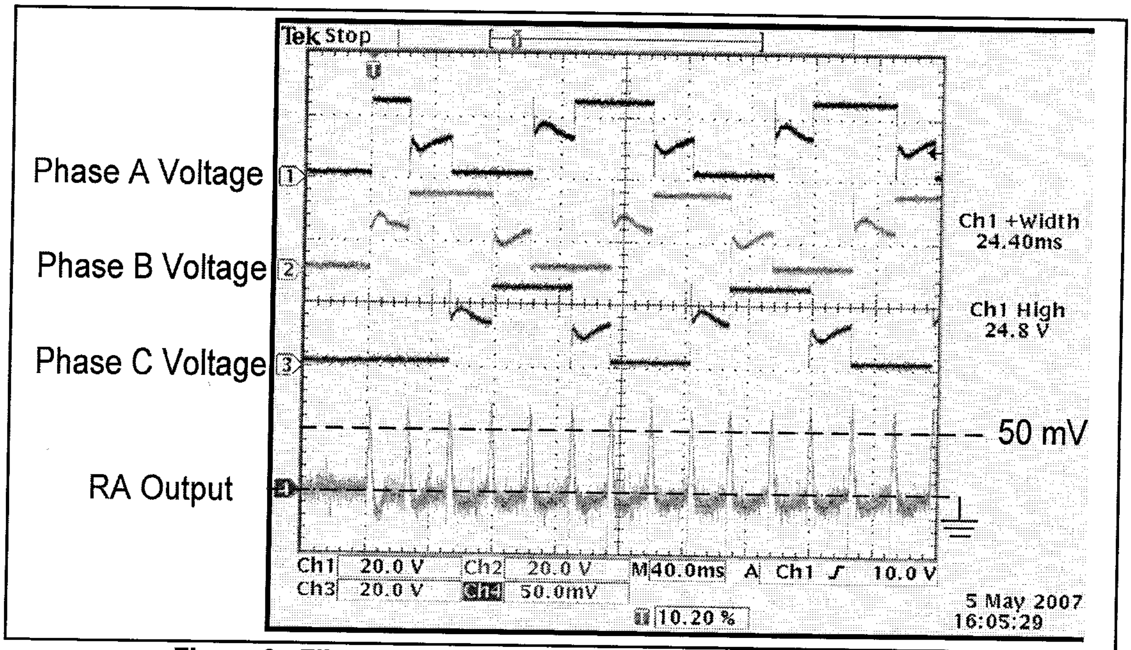

Figure 9. Flight Actuator Performance with Internal Damping

Table 4 delineates the difference in performance between the original, EDU#1, and the new, EDU#2 and Flight, units. From our kinematical analysis, we detail the differences in performance from our initial EDU#1 and "final" configuration. Most notable in the differences in performance, are the reduction in Peak Positional Overshoot, which reduced by 47%, and the Peak Velocity Overshoot, which reduced from -113 rad/sec (-1079 RPM), down to -22 rad/sec (-210 RPM). Since the kinetic energy varies with the square of the velocity, the Overshoot Velocity Kinetic Energy was reduced by an astonishing 96%.

Table 4. Motor Performance Comparison

Parameter	Units	EDU#1	EDU#2 and Flight	Comment
Power (Max)	Watts	29	25.6	At Maximum Voltage (34VDC), Lower = Better
Torque Margin	%	>400%	>200%	At Minimum Voltage (18VDC) Higher not necessarily better
Peak Positional Overshoot	**%**	**72%**	**25%**	**At Maximum Voltage (34VDC), Lower = Better**
Peak Velocity at Motor (during step transient)	rad/sec	161	108	At Maximum Voltage (34VDC), Lower = Better
Peak Velocity Overshoot at Motor	**rad/Sec**	**-113**	**-22**	**Kinetic Energy at Velocity Overshoot Reduced by 96%**
Reaction Torque at Load During Peak Acceleration	Nm	13.4	9.6	At Maximum Voltage (34VDC), Lower = Better

Drive Methods and Control Electronics

Method of Three-Phase Control

We decided to use three-phase stepper actuators, due to several tangible benefits such as fine step resolution, simple electronics with fewer power switching Field-Effect Transistors (FETs) and increased torque capacity under high friction conditions. There are many ways to control stepper motors, but the most common are wave and bipolar operation. Wave operation (also known as "Line-to-line" or 2/3 phase) and bipolar (also known as two-leads-tied or 3/3 phase) are represented in Figure 10 below.

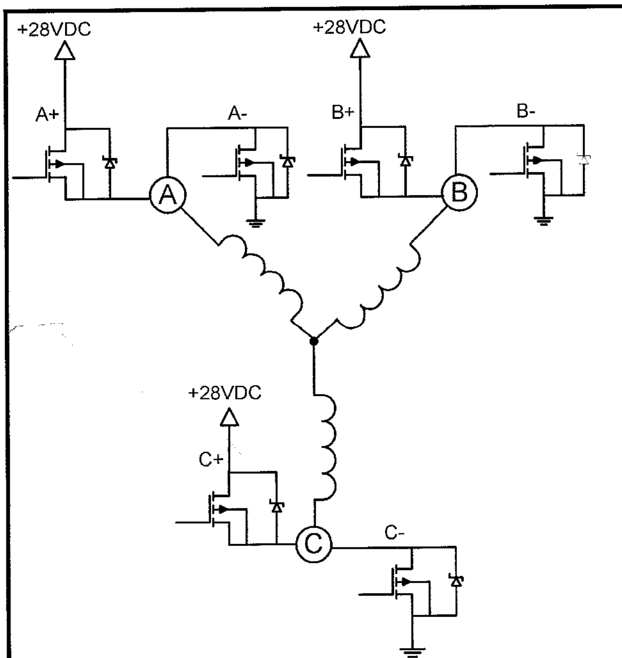

Wave Stepping Sequence						
Step	Active FETs					
	A+	A-	B+	B-	C+	C-
1	x			x		
2	x					x
3			x			x
4		x	x			
5		x			x	
6				x	x	
7	x			x		

Bipolar Stepping Sequence						
	Active FETs					
Step	A+	A-	B+	B-	C+	C-
1		x	x			x
2	x		x			x
3	x			x		x
4	x			x	x	
5		x		x	x	
6		x	x		x	
7		x	x			x

Figure 10: Three Phase Control Methods

For wave operation, two of the three phases are active at one time. In the Stepping Sequence Chart, we see that for the first step, Phase A is connected to the +28V through the A+ FET, and Phase B is connected to ground through the B- FET. Under this condition, current is flowing from A through B to ground. Phase C is open and is not connected through either FET. For the transition from step one to step two, Phase A remains connected to +28V, but now Phase C is connected to ground through C- FET and Phase B is open. The terminology of wave comes from this open leg shifting, and is analogous to two-phase wave operation. Referring back to **Figure 7**, this is a scope trace of the three phase stepping sequence of a wave drive with a regulated power supply. Notice how the voltage in the open leg oscillates during the overshoot transient. This is the back-emf circulating and causing the underdamped characteristics when no damping coils are present.

For bipolar operation, all legs are active during each stepping sequence. For bipolar step one, Phase B is "high" through the B+ FET, and both A and C are connected to ground through the A- and C- FETS respectively. At the second pulse, Phase B and C do not change state, but Phase A transitions from ground to +28V. This *controlled and continuous* reversal of current flow is why we call this method bipolar, and is analogous to two-phase bipolar operation.

Control Method Trades:

For either control method, during the transition of each pulse, you should *never* have the situation where the high and low side FETs of a common node (e.g. A+ and A-) are simultaneously active. If they were to be active at the same time, the current flow would bypass the motor and "shoot-through" from the supply voltage directly to ground, failing the FETs. Wave operation offers the advantage of not having to worry about "break-before-make" of the power stage FETs, while with bipolar operation you must "break" the active FET before "making" the next active FET. Therefore, the wave control method offers higher reliability and fewer failure modes compared to the bipolar operation. This was the discriminating factor in our selection of wave control for this space flight stepper motors.

An operational dilemma arises from the wave operation because there is an unregulated phase at each step, resulting in underdamped operation. For example, transitioning from step one to step two under the wave scenario, the current flowing in phase B is instantaneously cut-off from ground. At that instant, an L di/dt transient voltage is generated in reaction to the state change. The transient current flows through the B+ diode back into the supply voltage. Additionally, the motor back-emf generated from the stepper motion is allowed to flow freely in this unregulated winding, until step 3 when it is driven to the +28 voltage. The combination of the transient current and the back-emf result in an inherently underdamped control system. For bipolar operation, at each step of the control sequence all legs are actively controlled to either +28V or ground. There are no "free-wheeling" legs to allow transient currents to create an underdamped condition. This difference was found to be the root cause of the significantly underdamped condition of the mechanism.

Another observation of the various testing was the variation of performance whether the voltage supply was regulated or not. Notice the leg voltage measurements in Figures 3, 5 and 6. These voltages came from a non-regulated supply. You can clearly see the impact of the back-emf on the voltage during the step transient. Now notice the phase voltages on Figures 7 and 9. These voltages are generated on the regulated voltages in the control electronics. Notice the difference between the regulated and unregulated voltages during the step transients. The unregulated supply voltages "bounce" with the step transients, while the regulated voltages do not vary with the step transient. The differences in these voltage supplies will also affect the step characteristics; therefore, the voltage supplies used during testing should match the conditions the mechanism will see under flight conditions.

Processing the Rotary Accelerometer Signal

As previously discussed, we implemented an RA in the system for pulse step verification. The associated electronics to process the RA may be as sophisticated or as simple as desired, depending on the flexibility and capabilities required in the system. The charter for the RA in our system is pulse verification and state of health monitoring. For basic pulse verification a simple amplifier and comparator circuit is all that is required. An example of this circuitry is shown in Figure 11 [1]. The RA enables step verification by producing a voltage pulse that exceeds a specified threshold voltage each time the motor steps with the sign of the pulse indicating whether a clockwise or counter-clockwise step is taken. This method of step verification is called Original Transition Voltage Counting [1]. Figure 12 shows a single step of an adequately damped stepper motor system with a well defined pulse for step verification. This trace was actually taken by the actuator supplier of the EDU#1, driven at our nominal *power*, with a *bipolar drive configuration*. Notice the significant damping characteristic as compared to a single step of a wave controller, as shown in Figure 2, with equivalent power input.

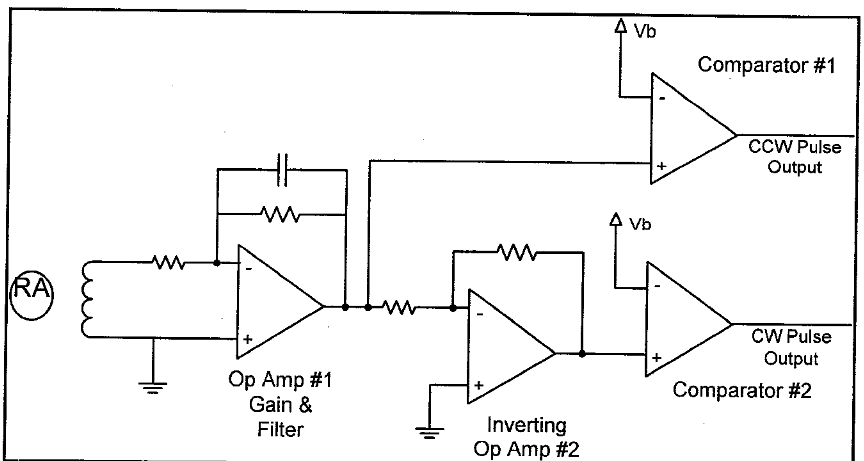

Figure 11. Simple Transition Voltage Counting Circuitry

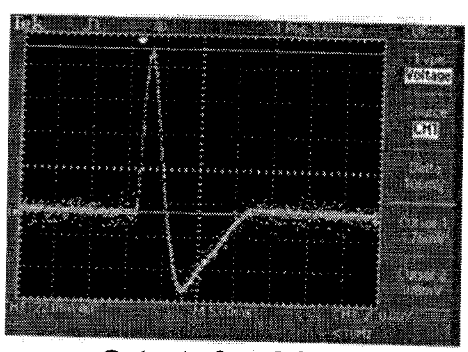

Figure 12. Oscilloscope Output of an Adequately Damped Single Step

Conclusion:

The first and most obvious conclusion is that EDUs proved invaluable to the process. EDU testing enabled the discovery of the underdamped condition at a stage in the process when corrective action did not negatively affect the program. Thanks to cooperation and teamwork between the Mechanisms, Electrical Engineering, System Engineering and Reliability Teams, as well as a responsive supplier, there was no impact to the program master schedule, even with a major in-process modification to the actuator.

The most significant lesson learned is that the drive control methodology and power supply regulation have a much more significant impact on mechanism performance than anticipated. Wave or unipolar drive methods result in a much more underdamped system, when compared to bipolar drive methods. Additionally, power supply voltages in test sets must duplicate on-orbit conditions, whether the supply is regulated or unregulated, because the supply voltage type affects the fundamental step kinematics and damping.

We discussed detrimental implications of an underdamped stepping mechanism, and the reasons to require an adequately damped system. We covered many common industry practices and potential options that could yield desired damping and mechanism characteristics. We took advantage of an excess of torque margin capacity within the motor, and used shorting coils to provide desired damping and mechanism performance. Our solution was efficient and robust, making use of existing technologies and capabilities while maintaining critical schedule requirements.

The utilization of a Rotary Accelerometer (RA) proved extremely useful in characterizing performance and troubleshooting potential solutions. Determining operational torque margin and conducting the simple kinematical analysis of the mechanism performance were also integral to the development and solution process. Utilization of an RA in the design increased mechanism reliability, improved position knowledge, verified step performance, and provided state of health information for this mission critical application.

Acknowledgements

Special thanks are extended to Erik Wilkinson, Charlie Hamp, Kiley Jones, Scott Miller, Richard Maxwell, Randall Whitaker, and the whole Mechanism, Electronics and Reliability teams at BATC that supported the testing, evaluation, review and solution process. Additional thanks and recognition go to CDA InterCorp for their responsive service and capabilities.

References

1. Starin, Scott, and Crosno, Fred, "System Characterization and Motor Step Verification through Rotary Acceleration Signals," 36th Aerospace Mechanisms Symposium, May 2002.

2. Starin, Scott and Neumeister, Jeff, "Eddy Current Damper Simulation and Modeling", Proc. 9th European Space Mechanism and Tribology Symposium, Liege 21 Sept. 2001, ESA SP-480, September 2001.

3. CDA InterCorp, "Stepper Motor Engineering Reference Data", © 2000

4. Ramakant Gayakwad and Leonard Sokoloff, "Analog and Digital Control Systems", Prentice Hall, Engelwood Cliffs, NJ 07632, © 1988.

5. Starin, Scott and Rodriguez, Tony, "Soft Stepping and Disturbance Compensation Through Rotary Acceleration Signal Processing" , Proc. 10th European Space Mechanism and Tribology Symposium, San Sebastian, Spain, 24-26 September, 2003, ESA SP-524, September 2003.